Nanostructured Pure γ-Fe_2O_3 via Forced Precipitation in an Organic Solvent

Abbas A. Khaleel*[a]

Abstract: Pure maghemite, γ-Fe_2O_3, was prepared as ultra fine particles in the nanometer-sized range via the forced precipitation method in an organic solvent. The precipitation of iron(III) ions, from iron(III) chloride in 2-propanol led selectively to highly dispersed particles of ferrihydrite, which upon treatment with temperatures higher than 200 °C under dynamic vacuum resulted in high-surface-area particles of γ-Fe_2O_3. Precipitation in water also led to ferrihydrite, but the final product, after heating at 300 °C, contained a mixture of γ-Fe_2O_3 and α-Fe_2O_3 (hematite). The precipitation from iron(III) nitrate in water resulted in goethite which was converted to hematite upon heating. On the other hand, the final product in 2-propanol was a mixture of maghemite and hematite. The products were characterized by FTIR, TGA, XRD, and gas sorption analysis. Nitrogen gas adsorption studies for the pure γ-Fe_2O_3 samples revealed mesoporous particles with high surface areas in the range of 70–120 m^2g^{-1} after heat treatment at 300 °C. The γ-Fe_2O_3 particles retained their γ-phase as well as their mesoporous structure at relatively high temperatures, as high as 400 °C.

Keywords: forced precipitation • hydrolysis • maghemite • mesoporous materials • nanostructures

Introduction

Metal oxides in nanometer-sized particles have attracted great attention in recent years due to the significantly unique properties which these materials exhibit compared with their bulk counterparts. The unique properties hold promises for remarkable performance in several important fields of applications including catalytic, magnetic, mechanical and biological applications.

In addition to the special interest to chemists for the significant role in catalysis, ultra fine powders of iron oxides are of great interest to physicists for their potential magnetic applications on which a wide range of technologies depend.[1–3] It has been well established that the performance of magnetic iron oxides is significantly improved by fabricating such materials from particles of average diameter below 50 nm (nanoscale particles), a behavior that is often referred to as nanomagnetism.[4]

On the other hand, iron oxides and iron oxides-containing composites have shown strong catalytic and adsorptive potentials in a variety of processes, including environmentally important reactions. Several studies have shown that iron oxides and composites containing iron oxides have a significant potential to adsorb and catalytically decompose volatile organic compounds[5,6] including chlorinated hydrocarbons.[7–9] In a previously patented work, we have discovered a unique catalytic behavior for iron oxides supported on high-surface-area magnesium oxide.[7] This potential catalyst was tested for the adsorption and decomposition of carbon tetrachloride where remarkable reactivity was found compared with that of pure magnesium oxide and other conventional catalysts. The unique catalytic behavior of iron oxides has driven our interest to investigate new methods to prepare nanometer-sized particles of iron oxides and composites containing iron oxides.

To date, the most widely studied chemical method to prepare iron oxides has been the precipitation of iron ions from aqueous solutions of their nitrate, chloride, perchlorate, or sulfate salts. This method has been reviewed and is well established in the literature.[10–15] The precipitation of ferric ions is usually driven by thermolysis or by the addition of a base to the aqueous solution. The product's phase and particle size have been found to depend on the precipitation conditions, especially the concentration of the iron ions, the nature of the counterions present, and the pH of the solution. Goethite (α-FeOOH), ferrihydrite ($Fe_5HO_8{\cdot}4H_2O$) or akagenite (β-FeOOH) are usually the initial precipitates, which are converted to crystalline low surface area α-Fe_2O_3 upon moderate heat treatment.[10,11,16,17]

The preparation of nanoscale particles of phase-pure iron oxides has been a real challenge due to the difficulties that usually accompany this process.[18–20] This is, in part, due to

---

[a] A. A. Khaleel
Department of Chemistry, UAE University
Al-Ain (United Arab Emirates)
Fax: (+971) 3-7671291
E-mail: abbask@uaeu.ac.ae

DOI: 10.1002/chem.200305135

the different iron oxidation states, which can lead to various oxides, FeO, Fe_2O_3, and Fe_3O_4. Moreover, Fe_2O_3 exhibits different phases, among which is hematite, α-Fe_2O_3, the most thermodynamically stable form. Finally, preparation of γ-Fe_2O_3 in nanometer-sized particles has been especially difficult due to the fact that it tends to aggregate into large particles, which makes the γ–α phase transition easier.[21] Several people have attempted to stabilize γ-Fe_2O_3 nanoparticles by dispersing them in polymeric[22,23] or ceramic matrices,[1,24–28] carbon nanotubes,[29] zeolites,[30] or by coating them with organic monolayers.[31,32] Besides the aqueous precipitation method,[13–15,17] other procedures to prepare nanostructured γ-Fe_2O_3 have been reported including microemulsion method[33,34] and decomposition of iron precursors.[35–38]

Herein we report the results of our recent work on the preparation of nanoparticles of pure γ-Fe_2O_3 via the precipitation of iron(III) ions in an organic solvent, 2-propanol.

Results and Discussion

Precipitation in aqueous versus alcohol solvents: The behavior of iron(III) ions in water has been well investigated and established in the literature.[7,8,20,21] The initial octahedral aqua complex of iron(III) which is formed in water, $Fe(H_2O)_6^{3+}$, instantaneously decomposes into several soluble low-molecular-weight species via deprotonation of coordinated water molecules. Some of the species which have been discussed include $[Fe(OH_2)_5(OH)]^{2+}$, $[Fe(OH_2)_4(OH)_2]^{+}$, and the dimeric species $[Fe_2(OH_2)_{10}(OH)_2]^{4+}$.[10,11] Further deprotonation and condensation of these intermediates usually lead to the formation of a soluble red cationic polymeric species, which was first isolated and characterized by Spiro et al. and was found to have a composition of the formula $Fe_4O_3(OH)_4(NO_3)_2 \cdot 1.5\,H_2O$, where nitrate was the counterion present in the solution.[39] The formation of this soluble polymeric species is promoted by adding a base in amounts insufficient to precipitate pure oxyhydroxides.[10,39]

In the current study, iron(III) chloride in water gave a stable yellow-gold clear solution showing no color change or any precipitate over a period of 5 d. The stability of the yellow-gold aqueous solution indicated that only low-molecular-weight soluble intermediates formed via deprotonation of coordinated water molecules, as indicated by the pH of the solution, which dropped from 5.4 for the pure water to 1.9 after the addition of $FeCl_3$.

The behavior of iron(III) ion in several alcoholic solvents was studied. In all systems the rate of the deprotonation and condensation process was dependent on the type of alcohol; however, in all of them it was significantly higher than that in water. This behavior was well indicated by the darker color of solutions and the deposition of precipitate in some cases. Water impurity from the solvents and atmospheric water was believed to play a role in the condensation and precipitation as a result of the formation of hydroxyl groups besides the alkoxy groups in the intermediate, which allows the elimination of alcohol molecules forming oxo bridges. The colors of the solutions ranged from orange to dark red. The intensities of the color and the rate of precipitate deposition increased as the alkyl group of the alcohol became larger. In methanol, a yellow orange solution was obtained initially, which developed to a darker orange solution over a period of 5 d without any precipitate. A dark red ethanol solution started depositing a precipitate very slowly after about 48 h. After five days, a small amount of red-brown precipitate and red solution was obtained. In 2-propanol fine red-brown precipitate started forming after ~8 h, and the solution was turbid red. When the 2-propanol solution was decanted and the precipitate was dried in a water bath at 90 °C, a red-brown powder was obtained. This powder was very soluble in water giving a red solution. The FTIR spectrum of this powder, as obtained, showed strong absorptions at 415 and 685 cm^{-1}. It was an amorphous powder showing no diffraction pattern in its XRD analysis.

When the same study was carried out using the nitrate precursor, $Fe(NO_3)_3 \cdot 9\,H_2O$, similar behavior was observed, but the deprotonation–condensation process was much faster. Darker solutions and larger amounts of precipitate were generally obtained, although the concentrations of the nitrate solutions were less than those of the chloride. It is very likely that this behavior is due to the presence of more hydroxyl groups in the soluble intermediate resulting from the water in the nitrate precursor. The red water-soluble product isolated from 2-propanol solution showed very similar FTIR absorption features with two major peaks at 660 and 436 cm^{-1}. The powder converted to ferrihydrite upon drying in an oven at 125 °C. When heated under vacuum at 300 °C for 4 h, the powder appeared to contain a mixture of hematite and maghemite as indicated from its FTIR spectrum (Figure 1), and powder XRD analysis. Its strong attractive magnetic behavior further supports the presence of the magnetic phase, maghemite. Their high solubility in water

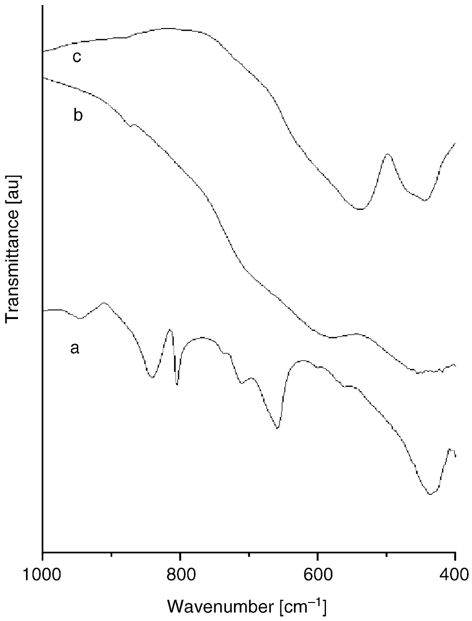

Figure 1. FTIR spectra of the soluble red polymeric alcoholysis product as obtained (a), after oven drying at 125 °C (b) and after heat treatment at 300 °C (c).

and their FTIR spectra indicated that these products were different from all known iron oxides or oxyhydroxides. These two characteristics of the products closely match those of the water-soluble product, $Fe_4O_3(OH)_4(NO_3)_2{\cdot}1.5\,H_2O$, isolated by Spiro et al., which has shown IR absorptions at 450 and 700 cm^{-1} attributed to oxy- and hydroxy-bent bridges.[40]

In conclusion, based on the comparisons discussed above, we believe that analogous to hydrolysis, alcoholysis took place via deprotonation of coordinated alcohol molecules. Further deprotonation and condensation of the soluble intermediates resulted into a precipitate without the need to add any base as a precipitating reagent, in contrast to the behavior in water. The precipitates obtained form both precursors and their thermal decomposition are the focus of an ongoing study but are believed to be analogous to that isolated in aqueous media by Spiro et al.[39,40]

Forced precipitation: Forced precipitation refers to the precipitation of metal ions by thermal treatment or by adding a base to their aqueous solution. As we have discussed in the previous section, hydrolysis of iron ions results in soluble intermediates, which upon adding a base, usually leads to α-Fe_2O_3, α-FeOOH, γ-FeOOH (lepidocrocite), $Fe_5HO_8{\cdot}4\,H_2O$ or β-FeOOH. The type of product depends mainly on the pH of the solution and the type of counterions present, that is, chloride, nitrate, sulfate, and so on.[10] At pH values between 4 and 10, hydrolysis of Fe^{3+} ions in aqueous solutions of iron(III) chloride has usually favored the formation of β-FeOOH instead of α-FeOOH (favored in the presence of other counterions).[10,16,20] In one study, this has been confirmed to be due to the presence of chloride ions, where the addition of some Cl^- to the solution of iron(III) nitrate during the aging of the red polymer has led to akaganeite, while the product was goethite in the absence of the chloride ions.[20] At pH values above 10 or below 4, goethite or hematite formed, respectively, even in the presence of chloride ions where akaganeite, if formed, converted to goethite or hematite.[41,42] All oxyhydroxides including goethite and ferrihydrite usually convert to hematite upon subsequent heating at temperatures above 200 °C.[10,17]

Interestingly, we found that forced precipitation of iron(III) ions in 2-propanol solution of $FeCl_3$ or $Fe(NO_3)_3{\cdot}9\,H_2O$ has led selectively to ferrihydrite ($Fe_5HO_8{\cdot}4\,H_2O$) with some unique characteristics. When a sodium *tert*-butoxide solution was added to the red solution of $FeCl_3$, red-brown fine precipitate formed. As discussed above, the red solution indicated the formation of soluble polymeric intermediates via deprotonation of coordinated alcohol molecules followed by condensation. The addition of the basic solution has resulted in the completion of the deprotonation and condensation process, where very fine precipitate and almost clear supernatant solution were obtained. Besides removing counterions, water which was added later was expected to hydrolyze all iron-coordinated alkoxy groups in the precipitate intermediate. The type of precipitate was found to be dependent on the type of the counterion present and on the solvent. Starting with $FeCl_3$, the product was selectively ferrihydrite in either solvent, 2-propanol or water. On the other hand, when $Fe(NO_3)_3{\cdot}9\,H_2O$ was used as the starting precursor, the product was always goethite in water while it was ferrihydrite in 2-propanol. Although both solvents have resulted in the same product using iron chloride, unique characteristics were observed when 2-propanol was employed. This includes higher surface areas and selective conversion to high-surface-area pure γ-Fe_2O_3 upon heat treatment at elevated temperatures as discussed below. The selective formation of ferrihydrite initially can be considered as an advantage since ferrihydrite is a poorly crystalline solid and is usually obtained as a high-surface-area powder compared with goethite (obtained from most other methods)[10,17] which strongly agglomerates into large particles or crystallites.

Ferrihydrite and goethite (dried in an oven at 125 °C) were characterized by FTIR spectroscopy and TGA analysis. The brown color of ferrihydrite is clearly different from the yellow color of goethite. The FTIR spectra of both compounds are shown in Figure 2. The absence of the goethite deformation band at 880 cm^{-1} in the ferrihhydrite spectrum indicates that it was free of goethite.

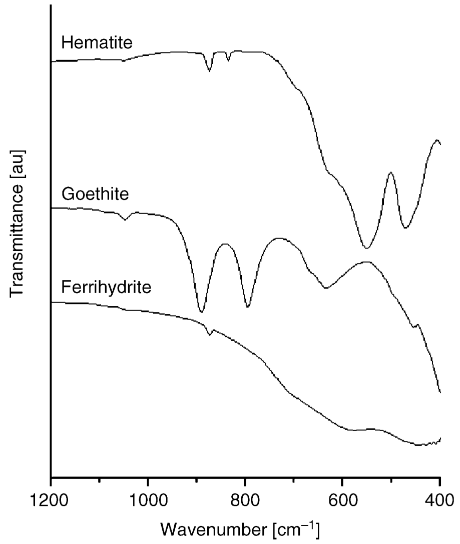

Figure 2. FTIR spectra of goethite obtained from an aqueous solution of $Fe(NO_3)_3{\cdot}9\,H_2O$, ferrihydrite obtained in 2-propanol solution of $FeCl_3$, and hematite obtained from the thermolysis of goethite at 300 °C in vacuo.

The TGA analysis (Figure 3) showed that the major weight loss in the case of ferrihydrite, which is due mainly to dehydration, took place at temperatures below 150 °C. This low-temperature weight loss can be due only to adsorbed water. This behavior again distinguishes ferrihydrite from goethite where the removal of structural hydroxyl groups (in goethite and other oxyhroxides) requires temperatures above 250 °C. Also, the larger final mass loss of about 21 versus 15 % for goethite further distinguishes ferrihydrite. This difference is due to the larger amount of water that can be removed from ferrihydrite of the formula $Fe_5HO_8{\cdot}4\,H_2O$ as compared with other forms of oxyhydroxides of the FeOOH formula. The XRD analysis showed no diffraction patterns as the samples were too amorphous.

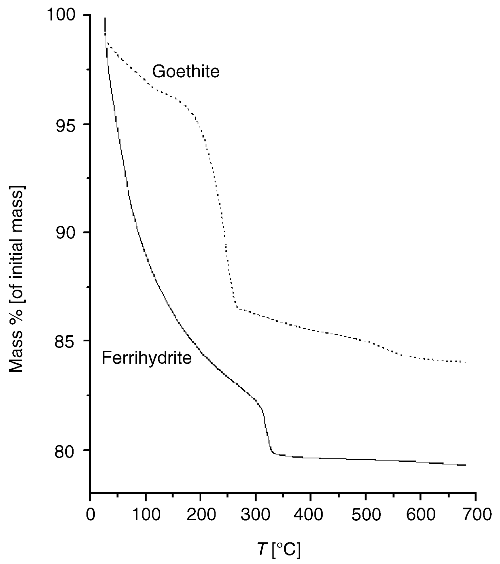

Figure 3. TGA analysis of ferrihydrite and goethite.

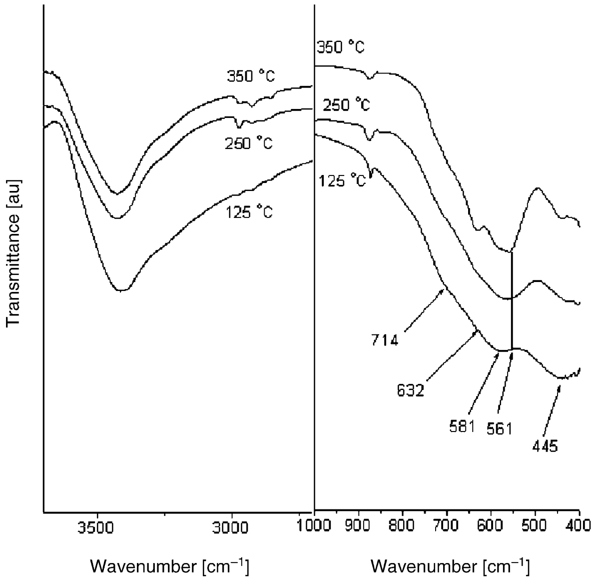

Figure 4. FTIR spectra of Ferrihydrite heat-treated at different temperatures under vacuum.

Heat treatment and phase transformations of goethite and ferrihydrite: All goethite samples converted to hematite when heat-treated under dynamic vacuum at 300 °C. This transformation was well indicated by the change in color from yellow to red, FTIR spectroscopy (Figure 2), and XRD analysis.

Ferrihydrite is known to transform easily to goethite or hematite upon heating.[10,17] In the current study, ferrihydrite prepared from $FeCl_3$ in 2-propanol converted to pure γ-Fe_2O_3 upon heating at temperatures between 200 and 350 °C. Ferrihydrite samples prepared from $Fe(NO_3)_3 \cdot 9\,H_2O$ in 2-propanol or from $FeCl_3$ in water have resulted in a mixture of α-Fe_2O_3 and γ-Fe_2O_3 as characterized by XRD. Besides the XRD analysis, the presence of the γ-phase was also confirmed by the fact that the product was attracted to a magnet, a characteristic of γ-Fe_2O_3 or Fe_3O_4, magnetite. The pure γ-Fe_2O_3 samples and their characteristics will be the main focus in the rest of this study.

The formation of pure γ-Fe_2O_3 was studied by FTIR spectroscopy where spectra were recorded for samples after heat treatment at different temperatures (Figure 4). Upon heating, the absorption bands centered at 445 and 714 cm^{-1} in the ferrihydrite spectrum decreased considerably in intensity while the peaks at 561, 581, and 632 cm^{-1} increased. These changes in the region of 400–700 cm^{-1}, indicated the gradual conversion to the typical spectrum of γ-Fe_2O_3.[17] Other notable features in the FTIR spectra are the absorption peaks between 2800 and 3000 cm^{-1}, and the strong $\tilde{\nu}$OH band centering at about 3430 cm^{-1}. These two features indicated the presence of relatively stable organic and hydroxyl groups, respectively, adsorbed on the surface after heating at 350 °C. We believe that the preservation of the organophilic species on the surface played an important role in determining some characteristics of the product, which will be discussed below.

Thermal decomposition of ferrihydrite to γ-Fe_2O_3 was also studied by powder XRD. Powder XRD analysis of a sample after heat treatment at 200 and 350 °C is shown in Figure 5. The diffraction patterns perfectly matched the data of the JCPDS file of γ-Fe_2O_3. Wide peaks in the pattern after heating at 350 °C indicated the significantly small size of the crystallites. The brown color of the powder further verifies that it was γ-Fe_2O_3 and not Fe_3O_4 (black) of the same spinnel structure and very similar XRD pattern. The fact that Fe_3O_4 transforms easily to γ-Fe_2O_3 at low temperatures, as low as 100 °C, further supports this conclusion.

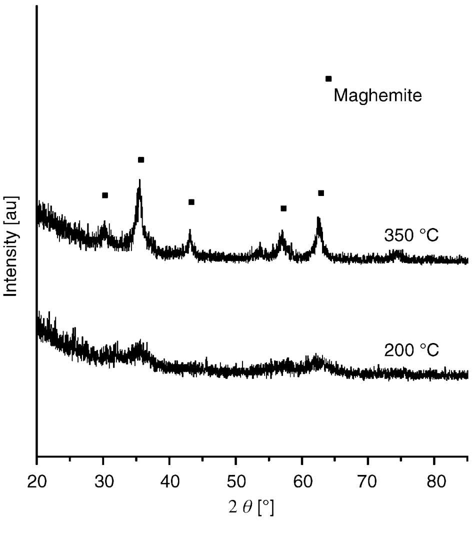

Figure 5. Powder XRD patterns for γ-Fe_2O_3 samples from ferrihydrite heat-treated at 200 and 350 °C.

TEM micrograph of a sample heat-treated at 250 °C showed aggregates of spherical primary particles with an average diameter of about 5 nm (Figure 6). Particle sizes estimated from TEM micrographs were in good agreement with crystallite sizes calculated by the Scherrer equation[43] based on XRD data.

Figure 6. TEM micrograph of a γ-Fe_2O_3 sample heat-treated at 250 °C.

N_2 Sorption analysis: One of the interesting characteristics of the samples prepared in 2-propanol was the relatively high surface area. Ranges of BET specific surface areas (SSA) measured for initial products, ferrihydrate or goethite, and heat treatment at 300 °C, are shown in Table 1. Three conclusions can be extracted from this data. First, it is noticed that for the initial products, higher surface areas are generally obtained from the 2-propanol solutions as compared with water. Second, ferrihydrite samples have shown much higher surface areas than goethite samples. Third, pure γ-Fe_2O_3 samples exhibited surface areas significantly higher than values reported in the literature.[1,17–20]

Table 1. BET specific surface areas [m^2g^{-1}] versus heat-treatment.

	$FeCl_3$		$Fe(NO_3)_3 \cdot 9H_2O$	
solvent	2-propanol	water	2-propanol	water
initial product[a]	ferrihydrite	ferrihydrite	ferrihydrite	goethite
SSA[a]	250–270	160–190	130–170	85–90
final product[b]	γ-Fe_2O_3	γ-Fe_2O_3 + α-Fe_2O_3	γ-Fe_2O_3 + α-Fe_2O_3	α-Fe_2O_3
SSA[b]	70–120	40–60	50–100	80–90

[a] Oven-dried at 125 °C for 4 h. [b] After heat-treatment at 300 °C under vacuum for 4 h.

It is obvious that the use of 2-propanol as a solvent played an important role in the relatively high surface areas of the ferrihydrite and maghemite samples. Ferrihydrite is known to form fine particles with high surface areas (larger than 150 m^2g^{-1}) and poor crystallinity.[10] Poor crystallinity is also known to be enhanced by the presence of organic solvents,[10] which corresponds to the high surface areas of samples we obtained in 2-propanol. The presence of organic groups in the coordination spheres of the iron ions of the starting soluble intermediates, as discussed in a previous section, is believed to have limited the nucleation of the primary particles through steric effect resulting in an unusually noncrystalline and high-surface-area ferrihydrite.

Furthermore, the remaining of stable organic moieties adsorbed on the surface at higher temperatures as indicated by the FTIR spectra (Figure 4, the region between 2800 and 3000 cm^{-1}) played a similar role during the heating/dehydration process that resulted into the conversion of ferrihydrite into high-surface-area maghemite. The presence of such species on the surface inhibited the sintering process by minimizing the contacts between reactive centers that otherwise would have led to adhesion of primary particles' surfaces.

Full N_2 adsorption–desorption isotherms were measured for γ-Fe_2O_3 samples pretreated at 300 °C. A typical isotherm is shown in Figure 7, which resembles an IUPAC H3 type with a well defined hysteresis loop indicating mesoporous material with mixed pore systems.[44] The desorption cumulative pore volume curve is shown in Figure 8 and the pore size distribution is shown in Figure 9. Total pore volume was 0.34 cm^3g^{-1} for all pores of diameter smaller than 103.5 nm. The pore size distribution in Figure 9 shows a predominant pore diameter around 8.8 nm.

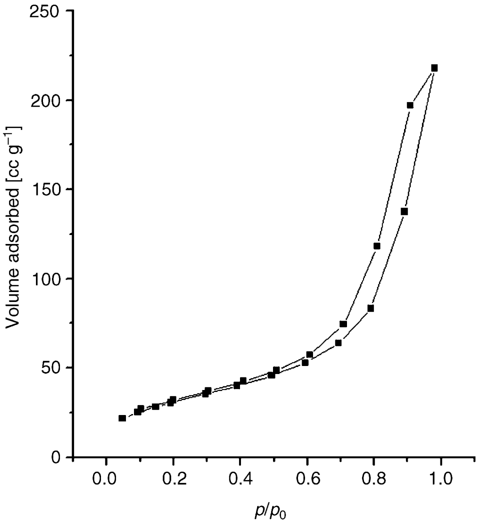

Figure 7. N_2 adsorption/desoprtion isotherm for a γ-Fe_2O_3 sample heat treated at 300 °C.

Changes in the surface area and pore characteristics were studied as a function of heat-treatment temperature. Table 2 shows the surface area, the total pore volume, and the average pore diameter of a sample after heating at different temperatures. The specific surface area decreased slightly as the sample was heated to 200 °C then decreased considerably as it was heated to 300 °C, beyond which a gradual decrease was observed. The effect of heating on the total pore volume was minimal, but generally a decrease was observed. On the other hand, a slight increase was observed in the average pore diameter upon heating. This behavior is usually due to sintering as a result of heating and subsequent dehydration resulting in bridging between primary particles and hence agglomeration into larger particles. This adhesion between outer surfaces of primary particles decreased the

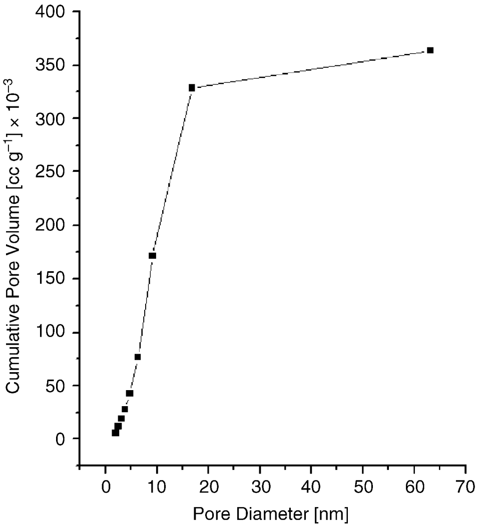

Figure 8. Desorption cumulative pore volume curve.

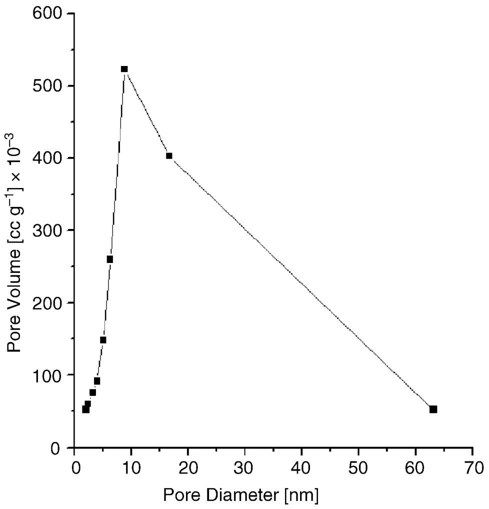

Figure 9. BJH pore size distribution; d*V*/d[logD] (desorption).

exposed surface and hence the surface area, while the pore structure was only slightly affected. With these changes in the surface area and porosity, the mesoporous structure was still preserved.

Another interesting characteristic of the nanoparticles of γ-Fe_2O_3 is their phase thermal stability where their γ-phase was retained at temperatures as high as 400 °C. Conventional γ-Fe_2O_3 is known to convert to the α-phase upon heating at temperatures above 250 °C.[45] Based on several literature reports, it is very likely that this high thermal stability, is due to particle size effect.[27,28,45–47] γ-Fe_2O_3 nanoparticles (~5 nm) encapsulated in silica matrix were found to retain their γ-phase after heat treatment at 700 °C.[27,28] In another study, upon preparation of nanocrystalline Fe_2O_3 through reverse micelle methods, it was found that below a crystal size of 30 nm only maghemite was produced while above this size, only hematite was obtained.[46] This dependence is still not well understood and it has been the subject of several studies.[46,48]

Table 2. Surface areas and pore characteristics of a ferrihydrite[a] sample heat-treated at different temperatures.

T [°C]	Surface area [m^{2}g^{-1}]	Total pore volume [cm^{3}g^{-1}]	Average pore diameter [nm]
125	260	0.32	7.9
200	215	0.34	10.9
300	114	0.33	11.8
350	102	0.30	12.2
400	93	0.30	12.5

[a] Converted to maghemite at $T > 200$ °C.

Mechanistic considerations in the γ-phase formation: α-Fe_2O_3, has been reported to be the most likely product from the thermal decomposition of pure ferrihydrite obtained from aqueous systems.[10,17] It is worth mentioning that the conventional method to prepare γ-Fe_2O_3 has been through reducing α-Fe_2O_3 to Fe_3O_4 which is then oxidized back to give γ-Fe_2O_3.[48] This procedure results in a crystalline γ-Fe_2O_3 of a surface area in the range of 20–30 m^{2}g^{-1}. From our discussion in the previous sections, it is obvious that among the factors that control the formation of the γ-phase are the type of solvent and the counterions. Under the current experimental conditions, the use of $FeCl_3$ precursor in 2-propanol has resulted in the formation of pure γ-Fe_2O_3, while all other routes have led to the formation of α-Fe_2O_3 or a mixture of γ-Fe_2O_3 and α-Fe_2O_3. It is evident that the chloride ions have played a major role in the γ-phase formation, which is still to be examined. On the other hand, the use of the organic solvent, 2-propanol, was another important determining factor that ensured the formation of pure γ-phase product. One possible role of the organic solvent is through the reducing effect of its carbonaceous residues during heating. These carbonaceous species may have caused partial reduction of Fe^{3+} ions giving magnetite (Fe_3O_4) which transforms to γ-Fe_2O_3 of the same spinel structure. The reducing effect of some organic species is well established in the literature, which allowed us to propose this role of the solvent in the γ-phase formation.[49–51] The oxidation of the divalent centers (in magnetite) back to trivalent (in maghemite) could be a result of possible generation of reactive oxidative species, for example, hydroxyl radicals from surface hydroxyl groups during heating.

Conclusion

The precipitation of iron(III) ions from iron(III) chloride in 2-propanol has led selectively to highly divided particles of ferrihydrite. Heat treatment at temperatures higher than 200 °C under dynamic vacuum has resulted in high-surface-area mesoporous particles of pure γ-Fe_2O_3. When the iron(III) nitrate precursor was employed under the same conditions, the final product, after heat treatment of the initial precipitate at 300 °C, was a mixture of α-Fe_2O_3 and γ-Fe_2O_3. On the other hand, employing water as the solvent resulted in pure α-Fe_2O_3 when the iron(III) nitrate precursor was used, while a mixture of α-Fe_2O_3 and γ-Fe_2O_3 was obtained in the case of the iron(III) chloride precursor.

The use of an organic media is believed to play an important role in the selectivity for γ-phase formation as well as in the high-surface area of the final product. The ultra fine powder of γ-Fe_2O_3 retained its γ-phase at relatively high temperatures, as high as 400 °C, which is believed to be due to particle size effect.

In comparison with literature reports, the following remarks can be highlighted. First, our simple synthetic procedure has resulted in pure nanoscale mesoporous particles of γ-Fe_2O_3, while most of the literature-reported work involved stabilizing the particles by dispersion into organic or inorganic matrices,[22–30] or by coating with relatively thick layer of organic additives.[31,32,49] Second, all studies that have been reported on the synthesis of pure γ-Fe_2O_3 involved extra steps such as the preparation of α-Fe_2O_3 first followed by vaporization condensation to convert it to the γ-phase,[38] or the preparation of Fe_3O_4 first followed by oxidation to γ-Fe_2O_3.[8,13] Direct precipitation in aqueous media under specific conditions has also resulted in γ-Fe_2O_3, but this method is very sensitive to experimental conditions especially the pH of the solution which makes the formation of impurities very likely to occur.[10,17] Third, in the current study smaller particle sizes and higher specific surface areas were obtained as compared to literature values of 10–50 nm particles and specific surface areas in the range between 30 and 50 $m^2 g^{-1}$.[8,13,17,35,38,52]

Experimental Section

Chemicals and instrumentation: $FeCl_3$ (anhydrous, 98 %), $Fe(NO_3)_3{\cdot}9H_2O$, sodium *tert*-butoxide (99 %), and 2-propanol (99 %), ethanol, and methanol (99 %) were purchased from Aldrich and used as received. FTIR spectra were recorded on a Nicolet Magna 560 spectrophotometer using KBr pellets. Powder x-ray diffraction analysis was performed on a Philips diffractometer model PW/1840 using a $Cu_{K\alpha}$ radiation source. Data was collected in the 2θ angle range of 20–85°. TGA analysis was performed on a TA 2950 instrument. TEM micrographs were obtained using a Philips 201 electron microscope. BET surface area and Barrett–Joyner–Halenda (BJH) cumulative pore volume and pore volume distribution measurements were obtained using nitrogen gas adsorption at 77 K employing a Quantochrome NOVA-1000 volumetric gas sorption instrument. Prior to the N_2 sorption analysis, all samples were heat-treated under vacuum at 120 °C for 15 minutes to remove physisorbed water.

Free precipitation of iron(III) ions in aqueous versus alcohol solvents: To compare the behavior of iron(III) ions in alcohol solvents with that in water without the addition of any precipitating reagent, anhydrous $FeCl_3$ (2.0 g, 0.012 mol) or $Fe(NO_3)_3{\cdot}9H_2O$ (2.0 g, 0.005 mol) was dissolved at room temperature in 2-propanol (100 mL), ethanol, methanol, or water in closed Erlenmeyer flasks under air. The behavior of each solution, in regards to color change and precipitate deposition was monitored for a period of five days. Precipitates obtained were characterized by FTIR spectroscopy and powder XRD.

Forced precipitation: In a typical experiment anhydrous $FeCl_3$ (1.62 g, 0.01 mol) or $Fe(NO_3)_3{\cdot}9H_2O$ (4.0 g, 0.01 mol) were dissolved in 2-propanol (150 mL), in a closed 500 mL round bottom flask, giving orange-red solutions. Sodium *tert*-butoxide (3.0 g, 0.03 mol) dissolved in ethanol (80 mL) was added drop wise over a period of 30 min. As the alkali solution was added, very fine colloidal orange-red particles started forming and the mixtures were stirred for additional four hours. The solutions were then allowed to stand for 12 h where orange-brown fine precipitates and slightly yellowish supernatant solutions were obtained. Doubly distilled water (150 mL) was added and the solutions were stirred again for an additional hour. The solutions were allowed to stand for another hour where complete precipitation and yellowish clear supernatant were obtained. The precipitates were vacuum-filtered, washed with three 25 mL portions of doubly distilled water and dried in an oven at 125 °C for 4 h. The dry products were grinded resulting in brown powders. Similar synthetic procedure was carried out in water under the same conditions. Some selected samples were heat-treated under dynamic vacuum at elevated temperatures. The products obtained were characterized by FTIR, XRD, TGA, TEM and N_2 sorption analysis.

Acknowledgement

The financial support from the United Arab Emirates University, grant number 10-2-11/01 is acknowledged with gratitude. I also thank Dr. Kenneth J. Klabunde at Kansas State University, USA, for several fruitful contacts and for the TEM micrographs that were done at KSU during a summer visit.

---

[1] H. Pardoe, W. Chua-anusorn, T. Pierre, J. Dobson, *J. Magn. Magn. Mater.* **2001**, *225*, 41.

[2] L. Babes, B. Denizot, G. Tanguy, J. Jeune, P. Jallet, *J. Colloid Interface Sci.* **1999**, *212*, 474.

[3] Y. S. Kang, S. Risbud, J. F. Rabolt, P. Stroeve, *Chem. Mater.* **1996**, *8*, 2209.

[4] C. M. Sorenson, in *Nanoscale Materials in Chemistry* (Ed.: K. J. Klabunde), Wiley, New York, **2001**, pp. 169–221.

[5] J. Bandara, J. A. Mielczarski, J. Kiwi, *Appl. Catal. B* **2001**, *34*, 307.

[6] H. Idriss, E. G. Seebauer, *J. Mol. Catal.* **2000**, *152*, 201.

[7] a) A. Khaleel, K. J. Klabunde, D. Park, *High Temp. Mater. Sci.* **1995**, *33*, 99; b) K. J. Klabunde, A. Khaleel, US Patent No. 5712219, **1998**; c) K. J. Klabunde, A. Khaleel, US Patent No. 5759939, **1998**; d) K. J. Klabunde, A. Khaleel, US Patent No. 5914436, **1999**; e) K. J. Klabunde, O. Kopper, A. Khaleel, US Patent No. 5914436, **2000**.

[8] P. D. Hooker, K. J. Klabunde, *Environ. Sci. Technol.* **1994**, *287*, 1243.

[9] N. Gamillone III, K. Adib, J. P. Fitts, K. T. Rim, G. W. Flynn, S. A. Joyce, R. M. Osgood, *Surf. Sci.* **2002**, *511*, 267.

[10] C. M. Flynn Jr., *Chem. Rev.* **1984**, *84*, 31.

[11] J.-P. Jolivet, *Metal Oxides Chemistry and Synthesis, From Solution to Solid State*, Wiley, New York, **2000**.

[12] L. Suber, D. Fiorani, P. Imperatori, S. Foglia, A. Montone, R. Zysler, *Nanostruct. Mater.* **1999**, *11*, 797.

[13] M. P. Morales, S. Veintemillas-Verdaguer, M. I. Montero, C. J. Serna, A. Roig, L. Casas, B. Martínez, F. Sandiumenge, *Chem. Mater.* **1999**, *11*, 3058.

[14] R. Massart, V. Cabuil, *J. Chim. Phys. Phys.-Chim. Biol.* **1987**, *84*, 967.

[15] J. Lee, T. Isobe, M. Senna, *J. Colloid Interface Sci.* **1996**, *177*, 490.

[16] E. A. Deliyanni, D. N. Bakoyannakis, A. I. Zouboulis, K. A. Matis, L. Nalbandian, *Microporous Mesoporous Mater.* **2001**, *42*, 49.

[17] U. Schwertmann, R. M. Cornell, *Iron Oxides in the Laboratory, Preparation and Characterization*, VCH, New York, **1991**.

[18] D. Vollath, D. V. Szabo, R. D. Taylor, J. O. Willis, K. E. Sickafus, *Nanostruct. Mater.* **1995**, *6*, 941.

[19] M. P. Morales, C. Pecharroman, C. T. Gonzales, C. Serna, *J. Solid State Chem.* **1994**, *108*, 158.

[20] E. Kroll, F. M. Winnik, R. Ziolo, *Chem. Mater.* **1996**, *8*, 1594.

[21] P. Ayyub, M. Multani, M. Barma, V. R. Plkar, R. Vijayaraghavan, *J. Phys. C* **1988**, *21*, 2229.

[22] B. Pejova, M. Najdoski, I. Grozdanov, A. Isahi, *J. Mater. Sci. Mater. Electron.* **2000**, *11*, 405.

[23] D. Prodan, V. V. Grecu, M. N. Grecu, E. Tronc, J. P. Jolivet, *Meas. Sci. Technol.* **1999**, *10*, L41–L43.

[24] T. Ida, H. Tsuiki, A. Ueno, K. Tohji, Y. Udagawa, K. Iwai, H. Sano, *J. Catal.* **1987**, *106*, 428.

[25] M. Guglielmi, G. Principi, *J. Non-Cryst. Solids* **1982**, *48*, 161.

[26] C. Chaneac, E. Tronc, J. P. Jolivet, *Nanostruct. Mater.* **1995**, *6*, 715.

[27] C. Cannas, D. Gatteschi, A. Musinu, G. Piccaluga, C. Sangregorio, *J. Phys. Chem. B* **1998**, *102*, 7721.
[28] G. Concas, G. Ennas, D. Gatteschi, A. Musinu, G. Piccaluga, C. Sangregorio, G. Spano, J. Stanger, D. Zedda, *Chem. Mater.* **1998**, *10*, 495.
[29] P. K. Pradhan, T. Toba, T. Kyotani, A. Tomita, *Chem. Mater.* **1998**, *10*, 2510.
[30] E. T. Wahuni, Y. Arryanto, B. Setiadji, J. Webb, W. Chua-Anusorn in *Adsorpt. Sci. Technol. Proc. Pac. Basin Conf.* (Ed.: D. D. Do), 2nd ed., World Scientific Publishing, Singapore, **2000**, pp. 653–657.
[31] A. K. Boal, K. Das, M. Gray, V. M. Rotello, *Chem. Mater.* **2002**, *14*, 2628.
[32] J. Rockenberger, E. C. Scher, A. P. Alivisatos, *J. Am. Chem. Soc.* **1999**, *121*, 11595.
[33] T. Liu, L. Guo, Y. Tao, Y. B. Wang, W. D. Wang, *Nanostruct. Mater.* **1999**, *11*, 487.
[34] V. Chhabra, A. N. Maitra, P. Ayyub, S. Chattopadhyay, *Mater. Lett.* **1996**, *26*, 21.
[35] X. L. Xu, J. D. Guo, Y. Z. Wang, *Mater. Sci. Eng.* **2000**, *B77*, 207.
[36] D.-H. Wu, D. Li, J. Yang, X-J. Yang, L-D. Lu, X. Wang, *Gongneng Cailiao* **2001**, *32*, 413.
[37] S. Martelli, A. Mancini, R. Giorgi, R. Alexandrescu, S. Cojocaru, A. Crunteanu, I. voicu, M. Balu, I. Morjan, *Appl. Surf. Sci.* **2000**, *154–155*, 353.
[38] B. Martínez, A. Roig, X. Obradors, E. Molins, *J. Appl. Phys.* **1996**, *79*, 2580.
[39] G. T. Spiro, S. E. Allerton, J. Renner, A. Terzis, R. Bils, P. Saltman, *J. Am. Chem. Soc.* **1966**, *88*, 2721.
[40] G. W. Brady, C. R. Kurkijan, E. F. X. Lyden, M. B. Robin, P. Saltman, G. T. Spiro, A. Teriz, *Biochemistry* **1968**, *7*, 2185.
[41] E. R. Landa, R. G. Gast, *Clays Clay Miner.* **1973**, *21*, 121.
[42] R. J. Atkinson, A. M. Posner, J. P. Quirk, *Clays Clay Miner.* **1977**, *25*, 49.
[43] A. F. Wells, *Structural Inorganic Chemistry*, 5th ed., Clarendon Press, Oxford, **1984**.
[44] R. S. Michail, E. Robens, *Microstructure and Thermal Analysis of Solid Surfaces*, Wiley, New York, **1983**.
[45] F. Monte, M. P. Morales, D. Levy, A. Fernandez, M. Ocaña, A. Roing, E. Molins, F. O'Grady, C. Serna, *Langmuir* **1997**, *13*, 3627.
[46] T. González-Carreño, M. Morales, M. Gracia, C. Serna, *J. Mater. Lett.* **1993**, *18*, 151.
[47] G. Schimanke, M. Martin, *Solid State Ionics* **2000**, *136–137*, 1235.
[48] S. Saito, *Fine Ceramics*, Elsevier, New York, **1988**.
[49] A. B. Bourlinos, A. Simopolos, D. Petridis, *Chem. Mater.* **2002**, *14*, 899.
[50] T. Sugimoto, Y. Wang, *J. Colloid Interface Sci.* **1998**, *207*, 137.
[51] K. M. Parida, J. Das, *J. Mater. Sci.* **1996**, *31*, 2199.
[52] A. Khaleel, A. Al-Nayeli, unpublished results.

Received: July 8, 2003
Revised: October 29, 2003 [F5135]